The Design of RF Bandpass $\Sigma\Delta$ Modulators with Bulk Acoustic Wave Resonators

Farakh Javid[1], Hassan Aboushady[1], Nicolas Beilleau[1] and Dominique Morche[2]
[1]LIP6-SoC Laboratory, University of Paris VI, Pierre and Marie Curie, Paris, France
[2]CEA-LETI, Grenoble, France

***Abstract*— This paper proposes a method to introduce BAW resonators in the loop of a Continuous-Time Sigma-Delta modulator. The method is based on the equivalence between the Noise-Transfer-Function of a conventional bandpass Discrete-Time Sigma-Delta and the Noise-Transfer-Function of a Continuous-Time BAW-based Sigma-Delta modulator with FIRDACs. The method is general and can be applied to BAW resonators with and without cancellation of the anti-resonance frequency. The Noise-Transfer-Function and the Signal-Transfer-Function of the BAW-based Sigma-Delta modulator are analyzed and compared with their Discrete-Time counterpart.**

I. Introduction

Nowadays, efforts are made to develop Software-Defined-Radio receivers which aim to directly digitize the RF signal from the antenna in order to obtain an easily programmable multi-standard receiver. One solution to achieve this goal is to use a RF front-end circuit based on bandpass $\Sigma\Delta$ modulator [1] (Fig.1). At RF frequencies, integrated LC resonators are usually used as loop filters in the $\Sigma\Delta$ modulator. Integrated LC resonators have a low quality factor which degrades the Signal-to-Noise Ratio (SNR), [2]. A circuit for quality factor enhancement is then needed to avoid SNR degradation [2]. This circuit increases noise, non-linearity and power consumption.

In [3] it is proposed to include a SAW resonator in a $\Sigma\Delta$ modulator loop. SAW resonators are passive components that naturally have high quality factor, thus they won't require additional power. However their main drawback is their non compatibility with CMOS technology. As a consequence the modulator described in [3] is implemented with an off-chip SAW resonator.

In this paper we propose to include a BAW resonator inside a $\Sigma\Delta$ modulator loop. BAW resonators have very high quality factors and are process compatible with silicon technologies [4], [5]. A systematic design procedure based on loop gain equivalence between a Discrete Time (DT) bandpass $\Sigma\Delta$ modulator and a Continuous Time (CT) bandpass $\Sigma\Delta$ modulator with BAW resonator is presented. This equivalence has been made possible through the use of feedback FIRDACs [6].

In section II, we give a brief comparison between conventional LC resonator and BAW one. In section III, the proposed DT to CT transformation technique is presented. In section IV, this technique is applied to two design examples and their simulation results are discussed. The conclusion is given is section V.

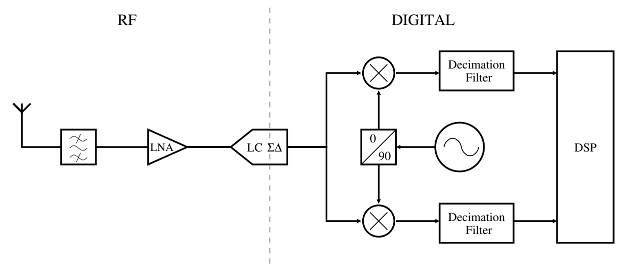

Fig. 1. RF receiver based on bandpass LC $\Sigma\Delta$ ADC.

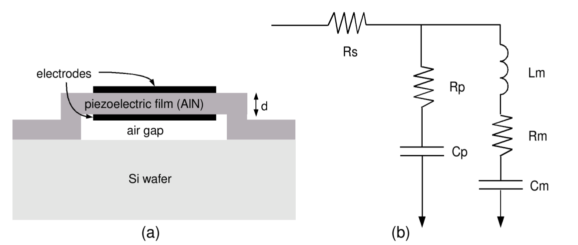

Fig. 2. (a) Physical view and (b) MBVD model of BAW resonator.

II. BAW resonators

BAW resonators are recent devices that work according to the piezoelectricity principle : an electrical signal applied to metallic electrodes is converted to a mechanical wave that moves into the piezoelectrical layer made of AlN (Aluminium Nitride) (Fig.2.(a)). Thus filtering operation is done mechanically. The center frequency of BAW resonator is given by : $f_0 = \frac{V_0}{2d}$ where d is the AlN thickness and V_0 the acoustic wave velocity in the piezoelectrical bulk. Two physical implementations for BAW resonators are possible: FBAR (Film Bulk Acoustic Resonator) and SMR (Solidly Mounted Resonator) which respectively use air gap and Bragg reflector to assure acoustic isolation [4]. Such an efficient isolation is the key to reach higher quality factor compared to LC resonator.

Now to study and simulate BAW resonator we use its electrical model named MBVD (*Modified Butterworth Van Dycke*). This model takes into account electromagnetic (R_p, C_p) and mechanical (R_m, C_m, L_m) behavior of BAW resonators [7] as shown Fig.2.(b). R_s models electrical loss due to metallic electrodes. The transfer function of MBVD model is given by

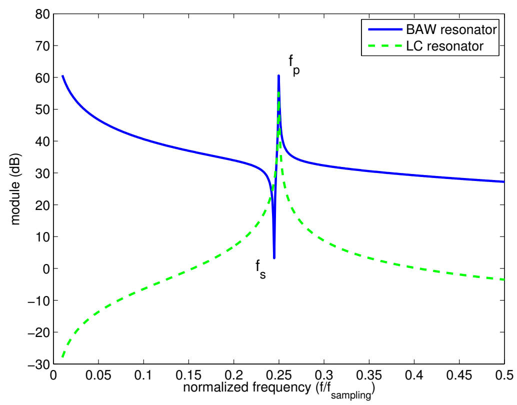

Fig. 3. LC and BAW resonator transfer functions for infinite Q, Q_{so} and Q_{po}. Normalized resonance frequency is at 0.25.

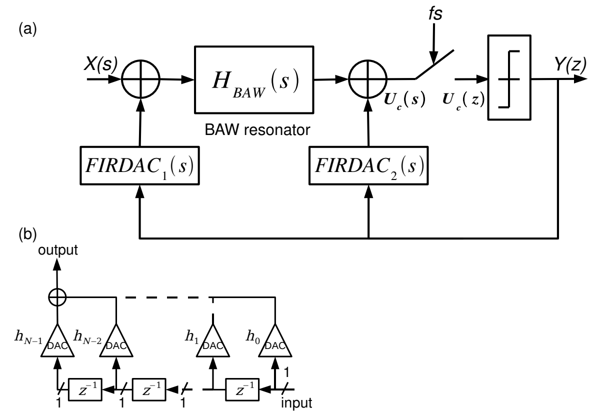

Fig. 4. (a) $\Sigma\Delta$ modulator with BAW resonator and FIRDACs and (b) one FIRDAC detail (N : number of coefficients in the FIRDAC) with $z^{-1} = e^{-Ts}$.

[8] :

$$H_{BAW}(s) = \frac{X_p \omega_p^3}{\omega_s^2} \frac{1}{s} \frac{s^2 + \frac{\omega_s}{Q_{so}} s + \omega_s^2}{s^2 + \frac{\omega_p}{Q_{po}} s + \omega_p^2} \tag{1}$$

with :

$$\begin{array}{ll} \omega_s = \frac{1}{\sqrt{L_m C_m}} & (\frac{\omega_p}{\omega_s})^2 = 1 + \frac{1}{r} \\ \frac{1}{Q_s} = \omega_s R_m C_m & \frac{1}{Q_e} = \frac{\omega_s R_p C_p}{r} \\ r = \frac{C_p}{C_m} & X_p = \frac{1}{\omega_p C_p} \\ \frac{1}{Q_{po}} = \frac{\omega_p}{\omega_s}(\frac{1}{Q_s} + \frac{1}{Q_e}) & \frac{1}{Q_{so}} = \frac{1}{Q_s}(1 + \frac{R_s}{R_m}) \end{array} \tag{2}$$

ω_p and ω_s are respectively resonance and anti-resonance pulsations. For comparison LC resonator's transfer function is :

$$H_{LC}(s) = \frac{\omega_0 s}{s^2 + \frac{\omega_0^2}{Q} s + \omega_0^2} \tag{3}$$

where ω_0 is the resonance pulsation. Both transfer functions are showed on Fig.3. We notice the presence of an anti-resonance frequency f_s near the resonance frequency f_p and a pole at the origin for the BAW resonator.

III. DT to CT transformation

In [6], the authors describe a method to design a CT modulator NTF from a DT one. Their method is based on the identification between CT and DT modulator loop gain and aims at computing CT modulator coefficients included in $FIRDAC_1$ and $FIRDAC_2$ (Fig.4.(a)).

The loop gain of a conventional second-order bandpass DT modulator is given by :

$$G_d(z) = \frac{1}{z^2 + 1} \tag{4}$$

According to Fig.4.(a) the CT loop gain is :

$$\begin{array}{ll} G_c(z) & = \frac{Y(z)}{U_c(z)} \\ & = Z\{H_{BAW}(s) FIRDAC_1(s) + FIRDAC_2(s)\} \end{array} \tag{5}$$

with :

$$\begin{array}{lcl} FIRDAC_1(s) & = & (\alpha_0 + \alpha_1 e^{-Ts} + \alpha_2 e^{-2Ts}) H_{DAC}(s) \\ FIRDAC_2(s) & = & (\beta_0 + \beta_1 e^{-Ts} + \beta_2 e^{-2Ts}) H_{DAC}(s) \\ H_{DAC}(s) & = & \frac{1 - e^{-Ts}}{s} \end{array} \tag{6}$$

where α_i and β_i are the coefficients in each FIRDAC. Assuming infinite Q_{so} and Q_{po} equation (1) becomes :

$$H_{BAW}(s) = \frac{K}{s} \frac{s^2 + \omega_s^2}{s^2 + \omega_p^2}, \quad K = \frac{X_p \omega_p^3}{\omega_s^2} \tag{7}$$

Including (6) and (7) in (5) we have :

$$\begin{array}{ll} G_c(z) = & (\alpha_0 + \alpha_1 z^{-1} + \alpha_2 z^{-2}) Z\{\frac{K}{s} \frac{s^2 + \omega_s^2}{s^2 + \omega_p^2} \frac{1 - e^{-Ts}}{s}\} \\ & + (\beta_0 + \beta_1 z^{-1} + \beta_2 z^{-2}) Z\{\frac{1 - e^{-Ts}}{s}\} \end{array} \tag{8}$$

Knowing that $Z\{1 - e^{-Ts}\} = 1 - z^{-1}$ and $Z\{\frac{1}{s}\} = \frac{1}{1 - z^{-1}}$ we get from equation (8):

$$\begin{array}{ll} G_c(z) = & (\alpha_0 + \alpha_1 z^{-1} + \alpha_2 z^{-2})(1 - z^{-1}) \underbrace{Z\{\frac{K}{s^2} \frac{s^2 + \omega_s^2}{s^2 + \omega_p^2}\}}_{A(z)} \\ & + (\beta_0 + \beta_1 z^{-1} + \beta_2 z^{-2}) \end{array} \tag{9}$$

Let's focus on $A(z)$:

$$A(z) = \underbrace{\frac{K}{\omega_p} Z\{\frac{\omega_p}{s^2 + \omega_p^2}\}}_{B(z)} + \underbrace{K Z\{\frac{\omega_s^2}{s^2(s^2 + \omega_p^2)}\}}_{C(z)} \tag{10}$$

Knowing $\omega_p = \frac{\pi}{2T}$ we find:

$$B(z) = \frac{K}{\omega_p} \frac{z}{z^2 + 1} \tag{11}$$

Using partial fraction expansion we obtain:

$$C(z) = \frac{K \omega_s^2}{\omega_p^3} \left(\frac{\pi z}{2(z-1)^2} - \frac{z}{z^2 + 1} \right) \tag{12}$$

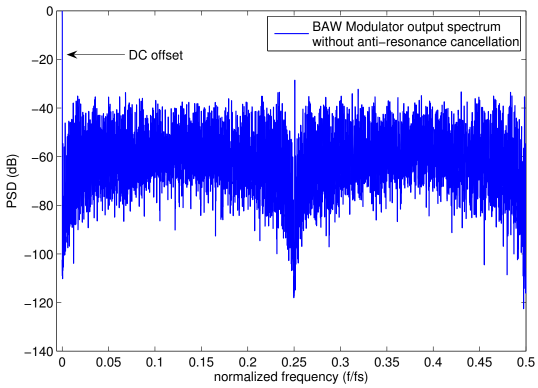

Fig. 5. $\Sigma\Delta$ modulator with BAW resonator output spectrum simulated (Matlab) with 16384 points, OSR=64, input amplitude=-23 dB, SNR=21.50 dB. Normalized resonance frequency is at 0.25. Notice DC offset on left side.

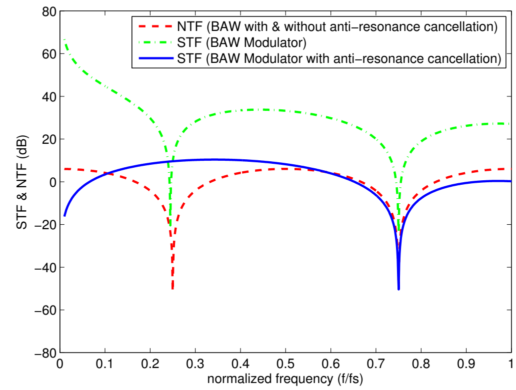

Fig. 6. STF of a $\Sigma\Delta$ modulator with BAW resonator with and without anti-resonance cancellation. NTF is the same for both BAW modulators and DT modulator. Normalized resonance frequency is at 0.25.

and then:

$$\begin{aligned} G_c(z) = \quad & (\alpha_0 + \alpha_1 z^{-1} + \alpha_2 z^{-2})(1 - z^{-1}) \\ & (\frac{K}{\omega_p}\frac{z}{z^2+1} + \frac{K\omega_s^2}{\omega_p^3}(\frac{\pi z}{2(z-1)^2} - \frac{z}{z^2+1})) \\ & +(\beta_0 + \beta_1 z^{-1} + \beta_2 z^{-2}) \end{aligned} \tag{13}$$

(13) can be written under the form :

$$\begin{aligned} G_c(z) = \quad & [K(\alpha_0 z^2 + \alpha_1 z + \alpha_2)((z^2+1) \\ & (\omega_p^2 + \frac{\pi}{2}\omega_s^2 - \omega_s^2) + 2z(\omega_s^2 - \omega_p^2))/\omega_p^3 \\ & +(\beta_0 z^2 + \beta_1 z + \beta_2)(z-1)(z^2+1)] \\ & /(z^2(z-1)(z^2+1)) \end{aligned} \tag{14}$$

Now we expect to solve:

$$G_c(z) = G_d(z) \tag{15}$$

$G_d(z)$ is modified to have the same denominator as $G_c(z)$ in order to equal their numerators and solve the equation. We set $z^2(z-1)(z^2+1)$ as common denominator. Then from equation (4) $G_d(z)$ becomes : $\frac{z^3 - z^2}{z^2(z-1)(z^2+1)}$.

To perform final calculations to get α_i and β_i values we use matrix representation of equation (15) described in [6]: $CF = D$, where C is a 6x6 matrix containing $G_c(z)$ numerator expression taken from equation (14) and rearranged according to z powers (rows) and α_i, β_i (lines), F and D are six lines rows respectively made of $G_c(z)$ numerator coefficients (α_i, β_i), and $G_d(z)$ numerator coefficients. At last, we have to solve $F = C^{-1}D$. Using a symbolic mathematical tool, we find the coefficients of the two FIRDACs in function of the parameters of the BAW resonator :

$$\begin{aligned} \alpha_0 &= \frac{\pi^3}{4KT(4\omega_s^2T^2 - \pi^2)} & \beta_0 &= 0 \\ \alpha_1 &= -\frac{\pi^3}{4KT(4\omega_s^2T^2 - \pi^2)} & \beta_1 &= -\frac{-4\omega_s^2T^2 + \pi^2 + 2\omega_s^2T^2\pi}{2(4\omega_s^2T^2 - \pi^2)} \\ \alpha_2 &= 0 & \beta_2 &= 0 \end{aligned} \tag{16}$$

IV. Design examples

In this section we present two design examples. The first design is a $\Sigma\Delta$ modulator using only a BAW resonator. The second one includes the anti-resonance cancellation system described in [3].

A. $\Sigma\Delta$ *modulator with BAW resonator*

We apply the method proposed in the previous section to design a bandpass second-order $\Sigma\Delta$ modulator with a BAW having a resonance frequency at 2 GHz ($R_s = 1.02\ \Omega$, $R_p = 0.85\ \Omega$, $R_m = 0.65\ \Omega$, $C_p = 1.8\ pF$, $C_m = 80\ fF$, $L_m = 79.4\ nH$, see Fig.2). In this case the coefficients of $FIRDAC_1$ and $FIRDAC_2$ are : $\alpha_0 = -0.26$, $\alpha_1 = 0.26$, $\alpha_2 = 0$, $\beta_0 = 0$, $\beta_1 = 18.17$, $\beta_2 = 0$.

As can be seen in Fig.5, simulation results show that noise shaping around f_p is not identical to a second-order bandpass $\Sigma\Delta$. We also notice a strong DC offset on the output spectrum of the BAW-based $\Sigma\Delta$. In fact, by comparing the NTF and STF of the designed BAW-based $\Sigma\Delta$ with its DT counterpart (Fig.6), we find that although the NTFs are identical, there is a significant difference in the STFs. This is mainly due to the anti-resonance and the pole at the origin. In this design, the maximum achievable SNR is only 21.5 dB (Fig.8).

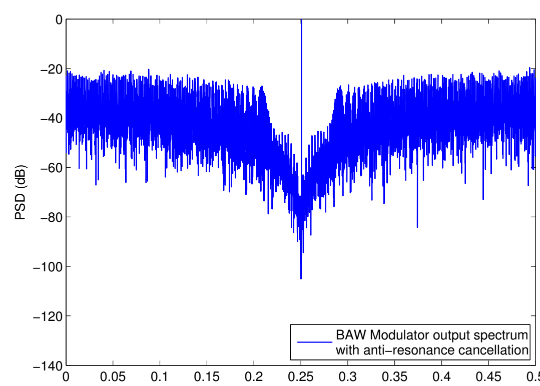

Fig. 7. $\Sigma\Delta$ modulator with BAW resonator and anti-resonance frequency cancellation output spectrum simulated (Matlab) with 16384 points, OSR=64, input amplitude=-1 dB, SNR=55.63 dB. Normalized resonance frequency is at 0.25.

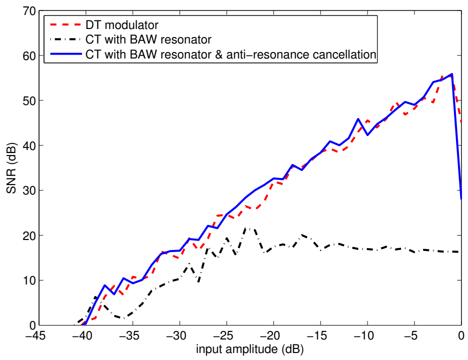

Fig. 8. SNR in function of input amplitude of a DT modulator and CT (with BAW resonator and infinite Q_{po} and Q_{so}), OSR=64, 16384 points. Peak SNR is 55.63 dB for BAW modulator.

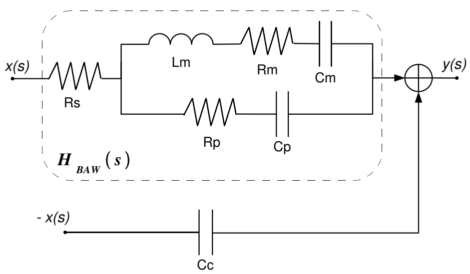

Fig. 9. $\Sigma\Delta$ modulator with BAW resonator and anti-resonance frequency cancellation capacitance C_c.

B. $\Sigma\Delta$ *modulator with anti-resonance frequency cancellation*

If we add a capacitance C_c with differential input in parallel with BAW resonator [3] (Fig.9) we have :

$$H_{BAW_c}(s) = H_{BAW}(s) - \frac{1}{sC_c} = \frac{K}{s}\frac{s^2+\omega_s^2}{s^2+\omega_p^2} - \frac{1}{sC_c} \quad (17)$$

Now giving C_c the same value as C_p and after simplifying equation (17) with equation (2) we get :

$$H_{BAW_c}(s) = \frac{s(C_m/C_p^2)}{s^2+\omega_p^2} \approx \frac{2\omega_p s}{s^2+\omega_p^2} \quad (18)$$

which is close to the LC resonator transfer function (equation (3)), and without the term representing the anti-resonance pulsation ω_s. FIRDACs coefficients are computed using the same technique described in section III by using the new expression $H_{BAW_c}(s)$ in symbolic mathematical program. We find the coefficients of $FIRDAC_1$ and $FIRDAC_2$ identical to those in equation (16) except for β_1 :

$$\beta_1 = -\frac{4\pi K C_c\omega_s^2T^2 - \pi^3 - 8KC_c\omega_s^2T^2 + 2KC_c\pi^2}{4KC_c(4\omega_s^2T^2-\pi^2)} \quad (19)$$

and then we have : $\alpha_0 = -0.26$, $\alpha_1 = 0.26$, $\alpha_2 = 0$, $\beta_0 = 0$, $\beta_1 = 0.5$, $\beta_2 = 0$.

The simulation now gives a better STF (Fig.6) without any DC offset (Fig.7) and the simulation results give an output power spectral density and a SNR identical to a DT second-order bandpass $\Sigma\Delta$ (Fig.8).

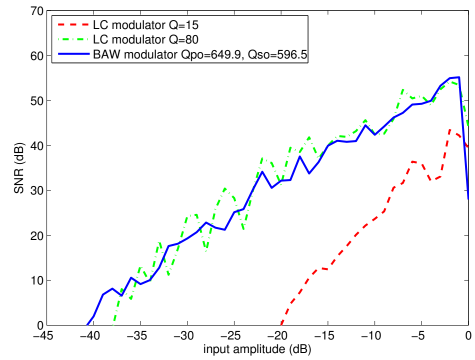

Fig. 10. SNR in function of input amplitude of LC modulator (with different Q factors) and BAW one (with anti-resonance cancellation and finite Q_{po} and Q_{so}), OSR=64, 16384 points. Peak SNR is 55 dB for BAW modulator.

In Fig.10 we plot SNR in function of input signal amplitude for LC and BAW modulators with finite quality factors. This graph shows that we have similar SNR for a LC modulator with active resistance (Q=80) and a BAW one (Q around 600). Therefore we reach LC modulator's best performance without adding any power consumption.

V. Conclusion

In this paper, we presented a general method for the design of a bandpass $\Sigma\Delta$ modulator with BAW resonator. The computation of FIRDACs coefficients is based on loop gain equivalence between DT and CT modulators. Two examples were designed and simulated. A technique to cancel anti-resonance frequency specific to BAW resonator was implemented and simulated, and greatly improves output spectrum and SNR.

References

[1] T. Chalvatzis, E. Gagnon, M. Repeta, and S.P. Voinigescu. "A Low-Noise 40-GS/s Continuous-Time Bandpass $\Sigma\Delta$ ADC Centered at 2 GHz for Direct Sampling Receivers". *IEEE Journal of Solid-State Circuits*, vol. 42(No. 5):1065–1075, May 2007.

[2] B. K. Thandri and J. Silva-Martinez. "A 63 dB SNR, 75-mW Bandpass RF Sigma-Delta ADC at 950 MHz Using 3.8-GHz Clock in 0.25-um SiGe BiCMOS Technology". *IEEE Journal of Solid-State Circuits*, vol. 42(No. 2):269–279, February 2007.

[3] R.R Yu and Y.Y.P. Xu. "Bandpass Sigma-Delta Modulator Employing SAW Resonator as Loop Filter". *IEEE Transactions on Circuits and Systems*, vol. 54(No. 4):723–735, April 2007.

[4] M.-A. Dubois, J.-F. Carpentier, P. Vincent, C. Billard, G. Parat, C. Muller, P. Ancey, and P. Conti. "Monolithic above-IC resonator technology for integrated architectures in mobile and wireless communication". *IEEE Journal of Solid-State Circuits*, vol. 41(No. 1):7–16, January 2006.

[5] S. Razafimandimby, C. Tilhac, A. Cathelin, A. Kaiser, and D. Belot. "An Electronically Tunable Bandpass BAW-Filter for a Zero-IF WCDMA Receiver". *European Solid-State Circuits Conference*, 2006.

[6] A. Kammoun N. Beilleau and H. Aboushady. "Systematic Design Method for LC Bandpass Sigma-Delta Modulators with Feedback FIRDACs". *IEEE International Symposium on Circuits and Systems*, May 2006.

[7] Eric Gaboriaud. *"Etude des résonateurs piézoélectriques dans le domaine des microondes : application au filtrage"*. PhD thesis, University of Limoges, France, 2004.

[8] J.D. Larson, P.D. Bradley, S. Wartenberg, and R.C. Ruby. "Modified Butterworth-Van Dyke Circuit for FBAR Resonators and Automated Measurement System". *IEEE Ultrasonics Symposium*, 2000.